# BENZOCYCLOBUTENE POLYMER IN GLASS MULTIMODE INTERFERENCE THERMO-OPTIC SWITCH

MASLINA YAACOB

UNIVERSITI TEKNOLOGI MALAYSIA

# BENZOCYCLOBUTENE POLYMER IN GLASS MULTIMODE INTERFERENCE THERMO-OPTIC SWITCH

MASLINA YAACOB

A thesis submitted in fulfilment of the
requirements for the award of the degree of
Master of Engineering (Electrical)

Faculty of Electrical Engineering
Universiti Teknologi Malaysia

JANUARY 2010

*Especially dedicated to my beloved parents, Yaacob and Hamidah,*
*my siblings and all my friend*
*for their prayers, warmth and support*

## ACKNOWLEDGEMENT

In the name of Allah, the Almighty and the Merciful…

Alhamdulillah, praise to Allah S.W.T for the guidance, strength and bless which He gave upon me to complete this research work.

I would first like to express my sincere gratitude and appreciation to my supervisor, Dr. Mohd Haniff Ibrahim for his advice, knowledge, supports, kindness and patience throughout this research work. I would also like to express my thanks to my co-supervisor, Assoc. Prof. Dr. Norazan Mohd Kassim and all Photonics Technology Centre members for their useful discussion, assistance and supports.

I am also indebted to Dr. Mohammad Faiz Liew Abdullah, Head of Optic Communication Laboratory, Universiti Tun Hussein Onn Malaysia (UTHM) and technician, Mr. Uzli Yusof for providing the accommodation at their lab for my simulation works.

I would also wish to acknowledge the Ministry of Science, Technology and Innovation (MOSTI) for their financial support through the National Science Fellowship (NSF).

Finally, special appreciation is dedicated to my family and friends for their constant support and prayers during my research work.

## ABSTRACT

Optical switch fabrics are integral parts of optically switched network because these devices are capable to direct input traffic to the appropriate output interface without resorting to optical-to-electrical-to-optical (OEO) conversion. This thesis is significantly devoted towards the design and simulation work of optical switch based on 2×2 multimode interference (MMI) coupler and exploiting thermo-optical properties of materials. Photosensitive BenzoCyclobutene (BCB 4024-40) polymer based coupler material was chosen due to its high thermo-optic coefficient, which offers less power consumption to induce thermo-optic effect in MMI coupler. The switching of the input signal to the desired output ports are realized by modifying refractive index at particular section of MMI coupler. Light propagation and thermal distribution through the optical switch are modeled by using a Finite Difference Beam Propagation Method (FD-BPM). In order to reduce the switching power, further analysis has been done by exploring the effect of heater's geometrical structure. It was observed that the employment of trapezoidal (tapered) heater structure can reduce the applied switching power by 15.53% as compared to the conventional rectangular structure. This improvement was shown to take place at crosstalk value of -19 dB. Significantly, this research has successfully demonstrated the application of tapered heater electrode in reducing the switching power for thermo-optic switch application.

## ABSTRAK

Suis optik adalah bahagian yang diperlukan dalam rangkaian suis optik kerana ia merupakan peranti yang berkebolehan menghalakan isyarat masukan kepada port keluaran dengan tepat tanpa melibatkan penukaran secara optik-elektrik-optik (OEO). Tesis ini secara khususnya memberi sumbangan kepada mereka bentuk dan simulasi suis optik yang berasaskan kepada pengganding gangguan berbilang mod (MMI) 2×2 dan mengeksploitasi kesan kawalan haba terhadap sifat bahan. Bahan pandu gelombang yang berasaskan polimer peka cahaya, BenzoCyclobutene (BCB 4024-40) telah dipilih berdasarkan pekali habanya yang tinggi, iaitu ia menawarkan penggunaan kuasa yang rendah bagi mendorong kesan kawalan haba di dalam pengganding MMI. Pensuisan isyarat masukan kepada port keluaran yang dikehendaki dapat direalisasikan dengan mengubah suai indeks biasan pada kawasan tertentu pengganding MMI. Perambatan cahaya dan taburan haba menerusi suis optik telah dimodelkan menggunakan kaedah perbezaan terhingga-perambatan alur (FD-BPM). Analisis lanjutan telah dijalankan dengan mengkaji kesan struktur geometri pemanas supaya penggunaan kuasa pensuisan dapat dikurangkan. Didapati bahawa penggunaan pemanas yang berstruktur runcing dapat mengurangkan penggunaan kuasa pensuisan sebanyak 15.53% berbanding dengan struktur segiempat yang biasa. Pembaikan ini telah menghasilkan cakap silang serendah -19 dB. Penyelidikan ini dengan jayanya telah menunjukkan aplikasi pemanas yang runcing dalam mengurangkan penggunaan kuasa pensuisan bagi aplikasi suis optik kawalan haba.

# TABLE OF CONTENTS

# LIST OF TABLES

# LIST OF FIGURES

## LIST OF ABBREVIATIONS

| | | |
|---|---|---|
| TEM | - | Transverse electromagnetic |
| TE | - | Transverse electric |
| TM | - | Transverse magnetic |
| MMI | - | Multimode interference |
| WDM | - | Wavelength division multiplexing |
| MPA | - | Mode propagation analysis |
| TO | - | Thermo-optic |
| FDM | - | Finite difference method |
| FEM | - | Finite element method |
| DC | - | Directional coupler |
| MZI | - | Mach-Zehnder interferometer |
| CT | - | Crosstalk |
| IL | - | Insertion loss |
| ER | - | Extinction ratio |
| EIM | - | Effective index method |
| BPM | - | Beam propagation method |
| ADI | - | Alternating direction implicit |
| TBC | - | Transparent boundary condition |

## LIST OF SYMBOLS

| | | |
|---|---|---|
| $R$ | - | Resistance |
| $E$ | - | Electric field |
| $H$ | - | Magnetic field |
| $J$ | - | Current density |
| $\rho$ | - | Charge density |
| $\sigma$ | - | Conductivity |
| $D$ | - | Electric flux density |
| $B$ | - | Magnetic flux density |
| $\varepsilon$ | - | Dielectric permittivity of the medium |
| $\mu$ | - | Magnetic permeability of the medium |
| $n$ | - | Refractive index |
| $\lambda$ | - | Wavelength |
| $k$ | - | Wave number of a medium |
| $N$ | - | Effective index of the mode |
| $\beta$ | - | Wave propagation constant |
| $\omega$ | - | Angular frequency |
| $\upsilon$ | - | Wave velocity |
| $v$ | - | Mode number |
| $d$ | - | Waveguide thickness |
| $L_\pi$ | - | Beat length of the two lowest-order modes |
| $c_v$ | - | Field excitation coefficient |
| $E(y,z)$ | - | Field profile |
| $L_{MMI}$ | - | Multimode waveguide length |
| $W_{MMI}$ | - | Multimode waveguide width |

| | | |
|---|---|---|
| $p$ | - | Periodic number of the imaging along the multimode waveguide |
| $\dot{Q}'''$ | - | Distributed thermal source per unit volume |
| $C$ | - | Specific heat |
| $t$ | - | Time |
| $k$ | - | Thermal conductivity |
| $P$ | - | Supply power |
| $w$ | - | Heater width |
| $h$ | - | Heater length |
| $I$ | - | Current through the heater electrode |
| $dn/dT$ | - | Thermo-optic coefficient |
| $\Delta n$ | - | Refractive index difference |
| $\Delta T$ | - | Temperature rise |

## LIST OF APPENDICES

# CHAPTER 1

# INTRODUCTION

## 1.1 Background of Research

Interest in optical communication began in mid-1960s, when early experiments showed that information encoded in light signals could be transmitted over a glass-fiber waveguide. Until the late 1990s, networks using optical fiber were viewed merely as transmission pipes that can carry a huge amount of traffic. Thus, the concept of integrated optics emerged in which the conventional electric integrated circuits are replaced by the photonic integrated circuits. In this all-optical communication system, the signal stays in the optical domain throughout the source–destination path. This implies that optical-electronic-optical (OEO) conversions are eliminated. The several application of optical switch in communication networks further increase the necessity of optical switch modules. As such, the switch are used inside optical cross connect to route optical signal in an optical network or system, allows the completion of traffic transmission in event of system or network failures by protection switching, switch functioning as optical add-drop multiplexers (OADMs) residing in network nodes insert (add) or extract (drop) optical channels (wavelength) to or from the optical transmission stream and optical switch that is used for signal monitoring verifying the proper operation of network element in term of wavelength accuracy, optical power levels and optical crosstalk.

In the past couple of years, the most widely investigated optical switches have been demonstrated by several structures such as directional coupler (DC) based

switch (Supa'at *et al.*, 2004), Mach-Zehnder interferometer (MZI) based switch (Inoue *et al.*, 1992), Y-branch based switch (Yeo *et al.*, 2006), multimode interference (MMI) based switch (Wang *et al.*, 2006) and combination of MMI-MZI based switch (Lai *et al.*, 1998). The configurations of these structures are illustrated in Figure 1.1. Among of this structures, MMI based switch are becoming more popular due to their excellent properties and easiness of fabrication. Their main advantages are ultra-compact size, low loss and large fabrication tolerances (Soldano and Penning, 1995).

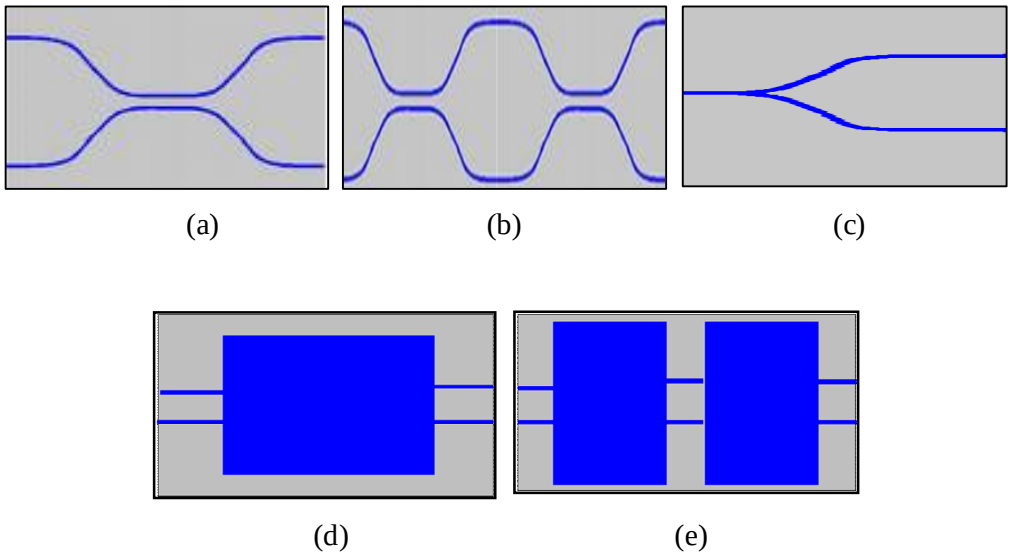


**Figure 1.1** Basic structures of optical switch (a) Directional coupler based switch (b) Mach-Zehnder interferometer based switch (MZI) (c) Y-branch based switch (d) Multimode interference based switch (MMI) (e) Combination of MMI-MZI based switch.

Recently, the most of tuning or switching methods of MMIs are based on the carrier-related electro-optic effect (May-Arrioja *et al.*, 2006) and thermo-optic effect (Moller *et al.*, 1993 and Al-hetar *et al.*, 2008). The MMI optical switches based on thermo-optic control are very attractive due to their simplicity and flexibility. The thermo-optic effect refers to the variation of the refractive index of a heated dielectric material. By tuning the refractive index directly within different sections of the MMIs, the refractive index modifications lead to the variations of the effective MMI

regions or the self-image phases within the MMIs which further realizing the switching operation.

Various materials such as semiconductor (Nagai *et al.*, 2002), silica (Sohma *et al.*, 2002), and polymer (Diemeer, 1998) have been used to fabricate planar lightwave circuits (PLCs). Recently, it has been reported that much interest have been devoted towards the application of hybrid polymer-silica integration technology in optical devices (Keil *et al.*, 2001 and Yeo *et al.*, 2006) This is due to the fact that both polymer and silica offer vast advantages in terms of low propagation loss (<0.1 dB/cm) (Wang *et al.*, 1996), low waveguide-to-fiber coupling loss (<0.05 dB) (Wang *et al.*, 1996), high fabrication throughput and employ low cost processing equipment (Eldada and Shacklette, 2000). Reviews on published optical switches are listed in Table 1.1.

**Table 1.1** Performance comparisons of optical switches

| Switch Configuration | Port | Material | Technology | Power/ Voltage/ Current | CT (dB) | Switching Time | IL (dB) | ER (dB) |
|---|---|---|---|---|---|---|---|---|
| MMI (Wang *et al.*,2006) | 1×2 | Polymer | Thermo-optic | 22 mW | -20 | - | - | - |
| MZI-MMI (Xia *et al.*, 2004) | 2×2 | SOI | Thermo-optic | 235 mW | - | 60 μs | 12 | 17.1 |
| MMI (May-Arrioja *et al.*,2006) | 2×2 | InGaAsp | Electro-optic | - | -20 | - | - | - |
| MMI (Wu *et al.*, 2006) | 1×2 | Sol-gel | Thermo-optic | 84 mW | - | - | - | 30 |
| MMI (Yin *et al.*, 2008) | 1×2 | GaAs/AlGaAs | Thermo-optic | 110 mA | -33 | - | - | - |
| MZI with 3 dB DC (Kasahara *et al.*, 2002) | 2×2 | Silica | Thermo-optic | 90 mW | - | 4.9 ms | 1 | 30 |
| Y-branch (Yeo *et al.*, 2006) | 1×2 | Hybrid polymer-silica | Thermo-optic | 70 mW | -35 | - | - | - |
| MZI-MMI (Liu *et al.*,2005) | 2×2 | SOI | Thermo-optic | 145 mW | - | 8 ± 1 μs | - | - |
| MMI (Thapliya *et al.*, 2008) | 2×2 | Polymer | Electro-optic | 3.8 V | -15 | 6 ns | - | - |
| MZI with 3 dB DC (Sohma *et al.*, 2002) | 2×2 | Silica | Thermo-optic | 45 mW | - | 3 ms | - | 35 |

| | | | | | | | | |
|---|---|---|---|---|---|---|---|---|
| MZI-MMI (Lai *et al.*, 1998) | 2×2 | Silica | Thermo- optic | 110 mW | - | 150 μs | 1 | 21 |
| MZI-MMI (Jin *et al.*, 2005) | 1×4 | Silica | Thermo- optic | - | -31.7 | | 1 | - |
| MZI with 3dB DC (Hida *et al.*, 1993) | 2×2 | Polymer | Thermo- optic | 4.8 mW | - | 9 ms | 0.6 | - |
| MMI (Nagai *et al.*, 2002) | 2×2 | InGaAsP | Electro-optic | - | -13 | - | - | 17 |
| Vertical coupler (Keil N. *et al.*, 2001) | 1×2 | Hybrid polymer-silica | Thermo- optic | 30mW | <−30 | - | 1.5 | - |
| MMI (Al-hetar *et al.*, 2008) | 2×2 | Polymer | Thermo- optic | 1.35 mW | -39 | < 1 ms | - | - |

**Notes:**

CT – Crosstalk

IL – Insertion loss

ER – Extinction ratio

## 1.2 Problem Formulation

High power consumption may increases the whole system's cost and the associated heat dissipation increase a system's ambient temperature, thus raising reliability issues (Papadimitriou *et al.*, 2007). It is utmost desirable for the developed optical switch to portray low switching power in order to meet current requirement of high speed and high capacity optical network. In this report, we focus in analyzing the effect of single heater electrodes in terms of geometrical structure to achieve low switching power consumption.

## 1.3 Objective of the Research

The research intends to develop 1×2 hybrid polymer-silica based MMI thermo-optical switch with low power consumption, high extinction ratio and low crosstalk. The research objectives can be specified as:

- To design a 2×2 MMI cross coupler as basic architecture of optical switch.
- To implement a hybrid polymer-silica based thermo-optic effect in designing MMI optical switch.
- To investigate the effect of heater electrodes in terms of geometrical structure towards power consumption, extinction ratio and crosstalk.

## 1.4 Scope of the Research

In order to fulfill the research objectives, the corresponding works to be carried out in this research are:

- Design and optimization of polarization-insensitive MMI cross coupler.
- Design and optimization of straight heater electrode in terms of size and position to obtain the optimum heater design for low power consumption.

## 1.5 Research Methodology

This research begins with literature studies on waveguide modeling techniques which include finite difference method (FDM), effective index method (EIM), and beam propagation method (BPM). The said methods are adopted in solving wave equation. Then, the literature review was followed by overview on multimode interefence (MMI) theory. The operation of MMI device based on self-imaging effect principle was explained in detail as presented in section 3.3.

Next phase will be on the studies of thermo-optic (TO) effect. This phase is required to understand the relationship of the parameters that governing the functionality of the switch. Simulations for thermal distribution analysis in optical waveguide will be carried out by using finite difference method (FDM) and finite element method (FEM) for comparison purpose. Thus, heat distribution in the optical waveguides can be obtained and eventually, better placement of heater electrodes can be designed in order to ensure excellent performance of the optical switch.

In order to develop MMI optical switch, a cross coupler has been adopted as basic architecture of switch structure. The simulation work will be based on BPM_CAD™ platform for multiple width and length combination of cross coupler. Further refinement was done in order to obtain a cross coupler structure with polarization-insensitive.

The crucial step in this project is to determine the structure and placement of heater electrodes. From literature, it was found that optical switch with low power consumption can be achieved by considering the size, shape and number of the heating electrode, as well as the

distance between heating electrode and core layer. Further simulation will be based on BeamProp™ software from RSoft® due to its versatility. This is because the BeamProp™ has advantages in designing active optical devices compared to BPM_CAD™ that only limit to passive optical devices design. From the simulation result, analysis will be carried out to obtain the required switching characteristics such as low switching power, low crosstalk and high extinction ratio. Finally, writing report in form of technical paper and thesis. The research methodologies are summarized in the following flow chart as shown in Figure 1.2.

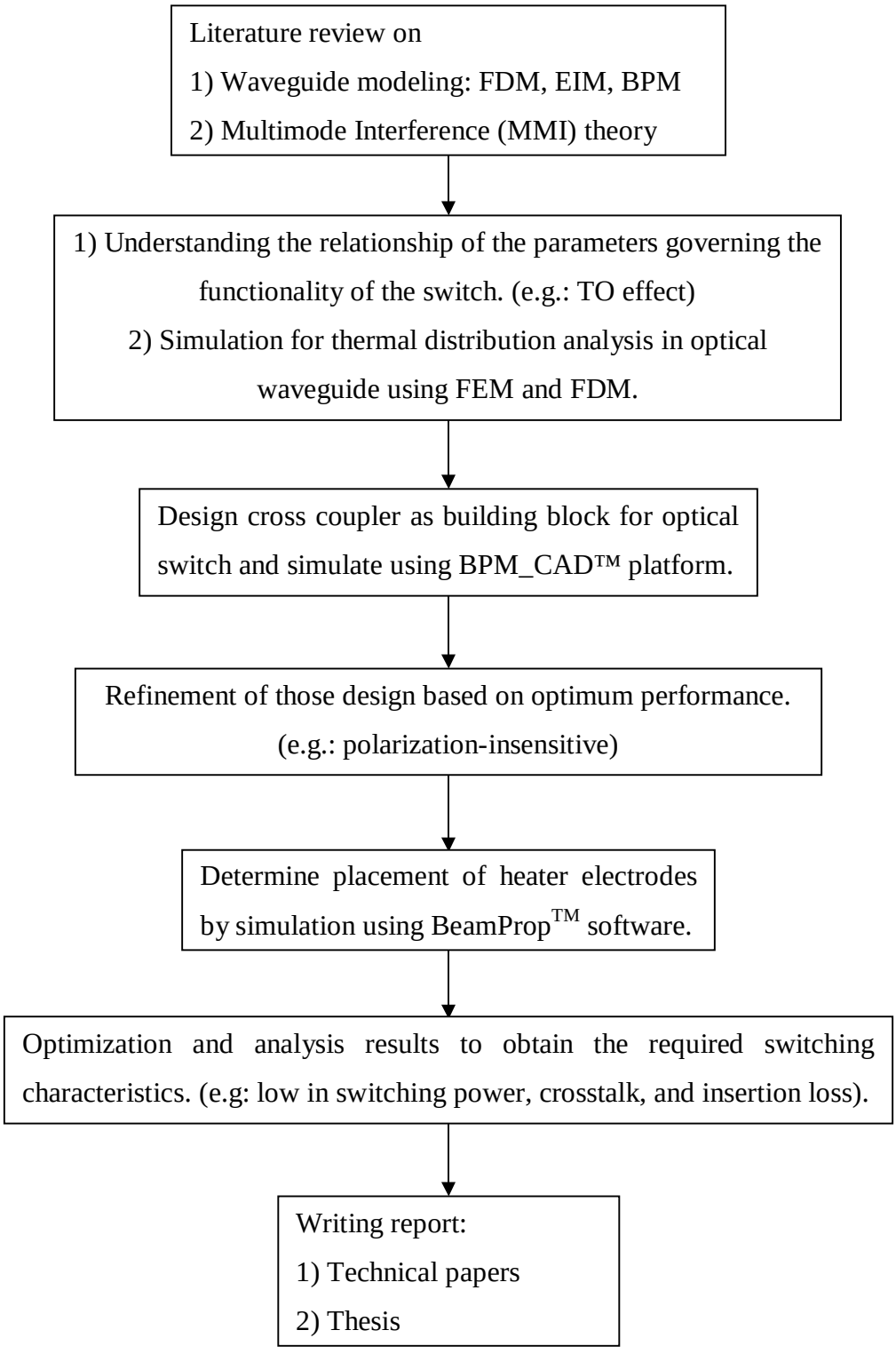


**Figure 1.2** The flow chart of research methodology

## 1.6 Overview of the Thesis

Chapter 1 presents an introduction of optical switch in optical communication networking. The objective and the scope of the research study are presented as well.

Chapter 2 discusses the main principles of optical waveguide theory. The general wave equation which describes the propagation of light in optical waveguide is derived using Maxwell's equation. The eigenvalue function for slab waveguide has been obtained using the ray-optics approach. The modeling techniques of channel waveguides have been discussed in detail, which include, the Effective Index Method, Finite Difference Method and Beam Propagation Method.

Chapter 3 explains the multimode interference (MMI) theory which is based on self-imaging principle. Classification on imaging mechanism into general interference and restricted interference has been explained in detail. The mathematical formulations that differentiate the properties of these interference mechanisms are briefly described.

Chapter 4 covers the thermal analysis which is the fundamental aspect in designing the optimum heater structure. A brief review of fundamental concepts, principles and basic equations in heat transfer are included in this chapter to understand how the guided modes can be controlled via thermo-optic effect. The temperature profiles of thermo-optic (TO) waveguides are analyzed by Finite Difference Method (FDM) and Finite Element Method (FEM).

Chapter 5 emphasizes on the simulation and optimization of the MMI TO switch. The optimization step starts from optimizing the MMI cross coupler by utilizing BPM-CAD software from OptiWave™. In order to design a TO switch and further analysis on heater's geometrical structure, the simulation was done by employing BeamProp software from RSoft®.

Finally, Chapter 6 remarks the overall conclusions and research contributions of this thesis and discusses possibilities for further development of this work.

# CHAPTER 2

# OPTICAL WAVEGUIDE THEORY

## 2.1 Introduction

This chapter reviews on optical waveguide theory which is fundamental in designing 2-D slab and 3-D channel optical waveguide. Also discussion on optical waveguide modeling based on effective index method (EIM), finite difference method (FDM) and beam propagation method (BPM).

## 2.2 Wave equation

Maxwell's equations are commonly written in the following form (Koshiba, 1992)

$$\nabla \cdot B = 0 \tag{2.1-a}$$

$$\nabla \cdot D = \rho \tag{2.1-b}$$

$$\nabla \times E = -\frac{\partial B}{\partial t} \tag{2.1-c}$$

$$\nabla \times H = J + \frac{\partial D}{\partial t} \tag{2.1-d}$$

where

$E$ = Electric field (V/m)

$H$ = Magnetic field (A/m)

$\rho$ = Charge density ($C/m^3$)

$J$ = Current density ($A/cm^2$)

From Ohm's law, current density can be stated as

$$J = \sigma E \tag{2.2}$$

where $\sigma$ is the conductivity (1 / Ωm). Assuming a lossless medium, the electric field $E$ and magnetic field $H$ are related to the electric flux density $D$ and magnetic flux density $B$ by

$$B = \mu H \tag{2.3}$$

$$D = \varepsilon E \tag{2.4}$$

where $\varepsilon_m$ and $\mu_m$ are the permittivity and permeability of the medium, respectively and can be further defined as

$$\mu = \mu_R \mu_O \tag{2.5}$$

$$\varepsilon = \varepsilon_R \varepsilon_O \tag{2.6}$$

where

$\mu_O$ = permeability of free space

$\mu_R$ = relative permeability of medium

$\varepsilon_O$ = permittivity of free space

$\varepsilon_R$ = relative permittivity of medium

Taking the curl of both sides of equation (2.1-c) gives

$$\nabla \times \nabla \times E = -\frac{\partial}{\partial t}(\nabla \times B) \tag{2.7}$$

Upon substituting equation (2.3) into equation (2.7) becomes

$$\nabla \times \nabla \times E = -\mu \frac{\partial}{\partial t}\left(\nabla \times H\right) \tag{2.8}$$

Substituting equation (2.1-d) into equation (2.8) gives

$$\nabla \times \nabla \times E = -\mu \left[\frac{\partial J}{\partial t} + \frac{\partial^2 D}{\partial t^2}\right] \tag{2.9}$$

Apply the vector identity

$$\nabla \times \nabla \times E = \nabla\left(\nabla \cdot E\right) - \nabla^2 E \tag{2.10}$$

to the left-hand side of equation (2.9) and substitute equation (2.2) and equation (2.4). If further simplify assume that $\sigma = 0$ and $\rho = 0$, then $\nabla \cdot E = 0$, we obtain

$$\nabla^2 E = \varepsilon\mu \frac{\partial^2 E}{\partial t^2} \tag{2.11}$$

Equation (2.11) is known as the *wave equation* and solving the *wave equation* for waveguide describes the modes of the waveguide mathematically.

## 2.3 2-D Slab Optical Waveguide

The simplest structure of optical waveguide is slab type as show in Figure 2.1. The slab is assumed to have the regions with refractive index of $n_c$, $n_g$, and $n_s$ which each refer to upper cladding, guiding region and substrate, respectively. Let the waveguide height be *d* and propagation in the *z* direction, the light being confined in the *x* direction by total internal reflection. The plane wave propagation constant in

the wave-normal direction is defined as $n_g k_0$ as shown in Figure 2.1, where $k_0 = 2\pi/\lambda_0$ and $\lambda_0$ is free space wavelength.

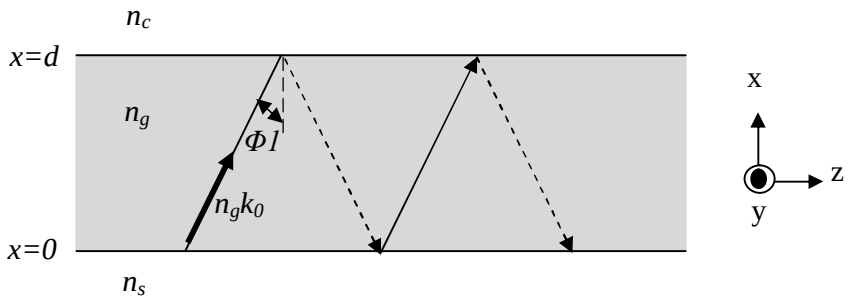


**Figure 2.1** Wave propagation in slab waveguide

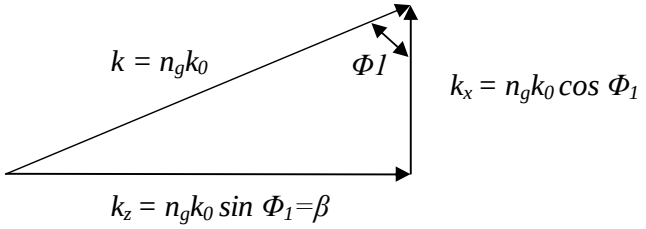


**Figure 2.2** Wave-vector diagrams

Regarding to Figure 2.2, $k$ can be decomposed into two components, in the $x$ and $z$ direction by simple trigonometry gives

$$k_x = n_g k_0 \cos \Phi_1 \tag{2.12-a}$$

$$k_z = n_g k_0 \sin \Phi_1 = \beta \tag{2.12-b}$$

Particularly, the propagation constant in the $z$ direction indicates the rate at which the wave propagates in the $z$ direction. $k_z$ is also known as $\beta$. Effective index, $N$ of the mode can be stated as

$$N = n_g \sin \Phi_1 \tag{2.13}$$

Thus equation (2.12-b) become

$$k_z = Nk_0 = \beta \tag{2.14}$$

Actually, the guided mode propagating along the *z* direction without 'zig-zaging' back and forth, with refractive index *N*. the corresponding range of *N* is

$$n_c > N > n_s \tag{2.15}$$

## 2.4 Eigenvalue Function in Slab Waveguide

In order to obtain eigenvalue in the waveguide structure, consider again the slab waveguide as shown in Figure 2.1. The field is uniform in *y*-direction, since the slab is assumed to be infinite in *y*-*z* plane. Slab waveguide can supports transverse electromagnetic (TEM) wave which contain of TE modes and TM modes. Here, we will solve the wave equation corresponding to TE modes since the similar analysis could be made for TM modes.

Based on above consideration, the *wave equation* (2.14) can be reduced to

$$\frac{\partial^2 E_y}{\partial x^2} + \frac{\partial^2 E_y}{\partial z^2} = \mu\varepsilon \frac{\partial^2 E_y}{\partial t^2} \tag{2.16}$$

Since there only electric field in y-direction, equation (2.16) can be written as

$$E_y = E_y(x) e^{j\omega t} e^{-j\beta z} \tag{2.17}$$

Differentiating equation 2.17 twice with respect to time, *t* and *z*-plane, we obtain

$$\frac{\partial^2 E_y}{\partial t^2} = -\omega^2 E_y \qquad (2.18\text{-a})$$

$$\frac{\partial^2 E_y}{\partial z^2} = -\beta^2 E_y \qquad (2.18\text{-b})$$

Substituting equation (2.18-a) and (2.18-b) into equation (2.16) gives

$$\frac{\partial^2 E_y}{\partial x^2} = \left(\beta^2 - \omega^2 \mu\varepsilon\right) E_y \qquad (2.19)$$

The following parameter can be defined

$$\text{Free space propagation constant, } k_0 = \frac{2\pi}{\lambda_0} = \frac{\omega}{c} \qquad (2.20)$$

$$\text{Wave velocity, } \upsilon = \sqrt{\frac{1}{\mu\varepsilon}} = \frac{c}{n} \qquad (2.21)$$

where $\lambda_0$ is free space wavelength, $\omega$ is angular frequency and $n$ is refractive index.

Hence, equation (2.19) can be simplified as (Reed and Knight, 2004)

$$\frac{\partial^2 E_y}{\partial x^2} = \left(\beta^2 - k_0 n^2\right) E_y \qquad (2.22)$$

The field solution and the boundary condition at the interfaces $x = d$ and $x = 0$ lead to *eigenvalue function* that determines the propagation characteristics of the TE modes and TM modes. From equation 2.22, the field solution are written in the form (refer Figure 2.1)

$$E_y = E_c \exp\left(-k_c x\right) \qquad , x > d \qquad \text{(in the cover)} \qquad (2.23\text{-a})$$

$$E_y = E_g \cos\left(k_x x + \Phi_c\right) \quad , d > x > 0 \quad \text{(in the waveguide)} \quad (2.23\text{-b})$$

$$E_y = E_s \exp\left\{k_s\left(x + d\right)\right\} \quad , x < 0 \quad \text{(in the substrate)} \quad (2.23\text{-c})$$

where the propagation constants are expressed in term of the effective index, *N* given by

$$k_c = k_0\sqrt{N^2 - n_c} \quad (2.24\text{-a})$$

$$k_x = k_0\sqrt{n_g{}^2 - N^2} \quad (2.24\text{-b})$$

$$k_s = k_0\sqrt{N^2 - n_s{}^2} \quad (2.24\text{-c})$$

The boundary condition that the tangential field components $E_y$ is continuous at the interface x=0 yields

$$E_c = E_g \cos\Phi_c \quad (2.25\text{-a})$$

$$\tan\Phi_c = \frac{k_c}{k_x} \quad (2.25\text{-b})$$

Similary, at $x = d$ yields

$$E_c = E_g \cos\Phi_c \quad (2.26\text{-a})$$

$$\tan\Phi_c = \frac{k_c}{k_x} \quad (2.26\text{-b})$$

Eliminating arbitrary coefficients in the preceding relation results in an *eigenvalue function*

$$k_x d = (v+1)\pi - \tan^{-1}\left(\frac{k_x}{k_s}\right) - \tan^{-1}\left(\frac{k_x}{k_c}\right) \quad (2.27)$$

where $v$ = 0, 1, 2,… represent the mode number. Thus, it indicated that propagation constant, $\beta$ can be obtained from equation (2.27) by knowing the refractive index of waveguide material and the guide thickness $d$. For the special case of the symmetric waveguide, where $k_c$=$k_s$, the *eigenvalue function* (2.27) can be simplified to

$$k_x d = (v+1)\pi - 2\tan^{-1}\left(\frac{k_x}{k_s}\right) \tag{2.28}$$

## 2.5 3-D Channel Optical Waveguide

Channel (3-D) waveguide are of immense importance in integrated optics, particularly in the context of integrated optic interconnection (Tocci and Caulfield, 1994). The slab waveguide in Section 2.3 guided lights in the $x$ direction, while the channel waveguide confines the optical modes in the $x$ and $y$ direction, thus a true optical interconnection structure can be formed. There are several types of channel waveguide, as shown in Figure 2.3.

The modal structure for channel waveguide is much more complicated to further separate modes on TE and TM compared to the case of slab waveguide (Tocci and Caulfield, 1994). Therefore, the effective-index method is a simple and fast approach to determine the propagation constant and effective index of channel (3-D) waveguide (Zeppe, 1995).

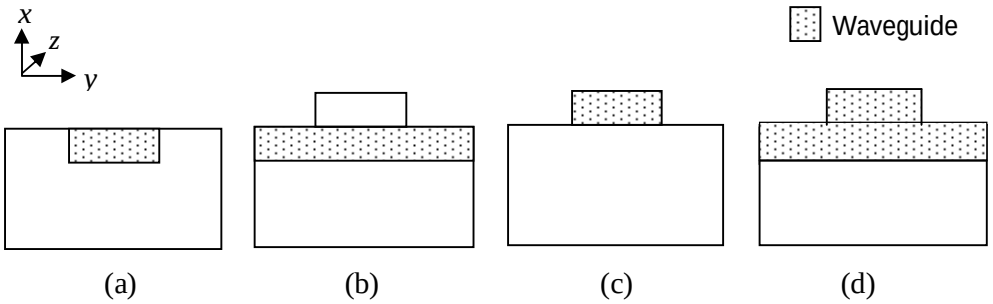


**Figure 2.3** Channel waveguide: (a) embedded strip; (b) strip loaded; (c) ridge; (d) rib

## 2.6 Effective Index Method (EIM)

Consider the channel (3D) waveguide with the rib type as shown in Figure 2.3(d). In effective index method, 3D optical waveguide is divided into region *I, II* and *III* as shown in Figure 2.4(a). Each region is then considered as 2D slab waveguide homogeneous in the *y* direction as shown in Figure 2.4(b). The effective index is then obtained by solving the *eigenvalue function* (equation 2.27) in *x* direction to produce $N_{eff\ 1}$, $N_{eff\ 2}$ and $N_{eff\ 3}$ for region *I, II* and *III*, respectively. Using the obtained effective index, the system can be further modeled as new 2D slab waveguide homogeneous in *x* direction as shown in Figure 2.4(c). By solving the *eigenvalue function* (equation 2.27) in *y* direction, the final effective index, *N* can be obtained. The propagation constant, $\beta$ can be calculated by using equation (2.14).

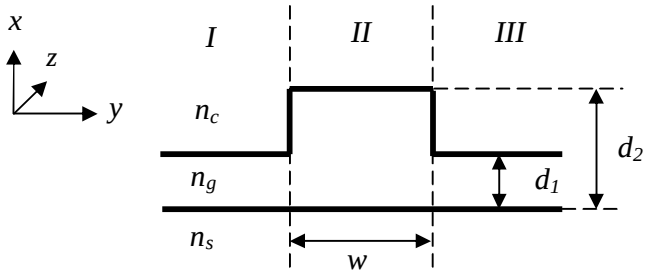


(a) Rib structure

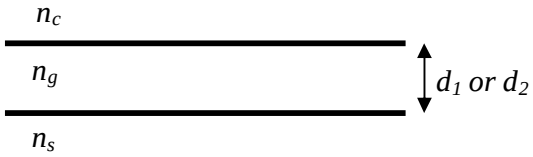


(b) 2D slab waveguide homogeneous in the *y* direction

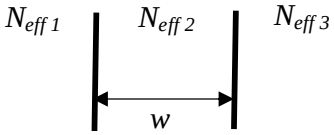


(c) 2D slab waveguide homogeneous in the *x* direction

**Figure 2.4** Effective index method diagram

## 2.7 Finite Difference Method (FDM)

Waveguide modeling can be divided into analytical and numerical technique. One of numerical technique is finite difference method (FDM). This method is popular due to its simplicity in the discretization procedure and the relative ease of implementation into a computer code. In the finite difference method, the governing equations are approximated by a point-wise disscretization scheme where derivatives are replaced by deference equations that involve the value of the solution at the nodal point (Majumdar, 2005). Finite different method illustration can be seen in Figure 1-A (Appendix A). Finite difference equation can be derived by using several approaches, which include Taylor series method or control volume method. The three point finite difference formula for the second derivatives can be state as

$$\frac{d^2E}{dx^2} = \frac{E(i+1, j) - 2E(i, j) + E(i-1, j)}{\Delta x^2} \tag{2.29}$$

By adopting equation (2.29), the scalar wave equation (2.16) can now be written in basic discretized form as (Ibrahim, 2007)

$$E(i, j) = \frac{E(i+1, j) + E(i-1, j) - 1}{2\left(1 + \left(\frac{\Delta x^2}{\Delta y^2}\right)^2\right) - \Delta x^2\left(k_0 n^2(i, j) - \beta^2\right)} \tag{2.30}$$

where $i$ and $j$ represent the mesh point corresponding to $x$ and $y$ direction respectively.

If Equation (2.16) is multiplied with $E$ and operating double integration towards $x$ and $y$, the Rayleigh Quotient will be obtained (Ibrahim, 2007)

$$\beta^2 = \frac{\iint Ey\left(\left(\frac{d^2E_y}{dx^2} + \frac{d^2E_y}{dy^2}\right) + k_0 n^2 E_y\right) dxdy}{\iint {E_y}^2 dxdy} \tag{2.31}$$

Thus, the propagation constant of the mode and electric field distribution in the waveguide can then be solved using numerical method based on equation (2.31).

## 2.8 Beam Propagation Method (BPM)

Beam propagation method (BPM) is one of the most popular numerical algorithms employed in modeling integrated and fiber optic photonic devices. BPM has proven to be an invaluable tool for the designer of integrated optic in the last decade (Benson *et al.,* 2007) and most commercial software for such modeling are based on it. After the introduction by Feit and Fleck (1980) to calculate the mode properties of optical fibers, the BPM has been applied to many waveguiding structures. The BPM is the most powerful technique to investigate linear and nonlinear lightwave propagation phenomena in axially varying waveguides such as curvilinear directional couplers, branching and combining waveguides, S-shaped bent waveguides, and tapered waveguides (Okamoto, 2006).

The BPM is based on the solutions of paraxial Helmholtz wave equation or known as Fresnel wave equation (Feit and Fleck, 1980). The basic approach is illustrated by formulating the problem under the restrictions of a scalar field (i.e. neglecting polarization effects) and paraxiality (i.e. propagation restricted to a narrow range of angles). The scalar field assumption allows the wave equation to be written in the form of the well-known Helmholtz equation for monochromatic waves:

$$\frac{\partial^2 \phi}{\partial x^2} + \frac{\partial^2 \phi}{\partial y^2} + \frac{\partial^2 \phi}{\partial z^2} + k(x, y, z)^2 \phi = 0 \qquad (2.32)$$

Here the scalar electric field has been written as $E(x, y, z, t) = \varphi(x, y, z)e^{-i\omega t}$ and the notation $k(x,y,z) = k_0\, n(x,y,z)$ has been introduced for the spatially dependent wavenumber, with $k_0 = 2\pi/\lambda$ being the wavenumber in free space. The geometry of the problem is defined entirely by the refractive index distribution $n(x, y, z)$.

It is possible to solve the paraxial wave equation using alternate numerical techniques. An alternate numerical scheme that solves the paraxial scalar wave equation is using a finite difference approximation (Chung and Dagli, 1990). The later work demonstrated that for most problems of interest in integrated optics, an implicit finite-difference approach based on the well-known Crank-Nicholson scheme was superior (Chung and Dagli, 1990). However, finite-difference for the three-dimensional problem is not a tri-diagonal equation as in the two-dimensional problems. Therefore, generally an inverse matrix operation is required. The following approximate solution method which is called *alternating-direction implicit finite difference method* (ADIFDM) can greatly simplify the calculation procedures (Okamoto, 2006).

The BPM is notoriously deficient in modeling structures that scatter radiation, since that radiation tends to reflect from the problem boundaries back into the solution region where it causes unwanted interference (Hadley, 1992). To avoid nonphysical reflection from the boundaries of the computational domain, transparent boundary conditions are employed (Hadley, 1992). In the TBC method, the electric field at the boundary is assumed to be expressed by the plane wave (Okamoto, 2006). The transparent boundary conditions (TBC) are superior to the conventional absorbing boundary conditions because they are more efficient and accurate. The transparent boundary conditions are shown to be highly effective in absorbing the outgoing waves, leading to more accurate results with less computation effort. Another advantage of the transparent boundary conditions is their robustness, i.e., that they are relatively independent of the waveguide structures (Huang *et al*., 1992). Moreover, the transparent boundary condition is also applicable in ADIFDM. Thus, three-dimensional BPM analysis can be efficiently performed by using ADIFDM (Okamoto, 2006).

The FDBPM technique has undergone extensive development since its first introduction such as wide-angle propagation via Pade approximation (Benson *et al.*, 2007). The essential idea behind this approach is to reduce the paraxiality restriction on the BPM (Bekker *et al.*, 2009).

## 2.9 Conclusion

The theoretical background for 2D-slab and 3-D channel optical waveguide has been described in this chapter, which is important to obtain and solve for the propagation constant value, $\beta$ that explained the behavior of propagated modes inside the optical waveguide structure. The discussion has been extended to the waveguide modeling techniques which include the Effective Index Method (EIM), Finite Difference Method (FDM) and Beam Propagation Method (BPM).